Plant Physiol. (1981) 67, 1016–1025
0032-0889/81/67/1016/10/$00.50/0

Morphology and Ultrastructure of Maternal Seed Tissues of Soybean in Relation to the Import of Photosynthate

Received for publication May 27, 1980 and in revised form November 7, 1980

JOHN H. THORNE[1]
Department of Ecology and Climatology, The Connecticut Agricultural Experiment Station, New Haven, Connecticut 06504

ABSTRACT

Cytological observations were made on developing seeds of soybean (*Glycine max* (L.) Merr. "Amsoy 71") using scanning and transmission electron microscopy and light microscopy. Attention was focused on the maternal tissues of the seed coat and embryo sac. An hypothesis of photosynthate import, unloading, and movement to the embryo is presented based on the results of these studies.

The agronomic productivity of soybean plants is dependent upon their capacity to partition a significant proportion of assimilates to the seeds. Indeed, the principal sink for phloem-translocated photosynthate in reproductive soybeans is the seed (20), and large amounts are imported to provide the energy requirements of seed growth and establishment of cotyledonary reserves. Recent kinetic and biochemical studies have presented an overview of photosynthate import within soybean fruit (22, 23). These identify the transport role of the seed coat and suggest that specialized transport processes may control the uptake of sucrose by developing soybean seeds (23). They trace the route of photosynthate transport (23), but provide no cellular or ultrastructural information for the evaluation of physiological controls. Although some aspects of the vascularization of developing legume fruit have been described in other studies (2–4, 7, 10, 17), a comprehensive investigation is lacking, especially with respect to the overall import of photosynthate. The present study was undertaken primarily to describe the anatomical structure of the maternal tissues of the soybean seed coat and embryo sac in an attempt to determine the probable pathway(s) of photosynthate transport from the vascular supply of the pod to the site of absorption by the embryonic cotyledons.

MATERIALS AND METHODS

Plant Culture. Nodulated plants of soybean (*Glycine max* (L.) Merr. "Amsoy 71") were grown in a controlled environment room in which illumination (1.5×10^3 μE m^{-2} s^{-1} PAR) was provided by a mixture of incandescent and Sylvania GRO-LUX wide-spectrum fluorescent lamps. Principal growth conditions (30/17 C, 14-h photoperiod) were interrupted from 45 to 60 days after planting to induce flowering (30/17 C, 9-h photoperiod). Seeds were harvested 45 to 50 days after flowering, prior to maximum fresh and dry weight.

Scanning Electron Microscopy. Freshly harvested seeds were submerged, dissected, and then fixed at 4 C for 1.5 h in 5% (v/v) glutaraldehyde containing 100 mM phosphate buffer (pH 7.0). After two 15-min rinses in phosphate buffer, tissue samples were postfixed for 1.5 h in 1% (v/v) osmium tetroxide containing 100 mM cacodylate buffer (pH 7.0). Following slow dehydration through a graded ethanol series, samples in absolute ethanol were dried using the critical point method of Anderson (1), vacuum-desiccated at room temperature, fractured, attached to specimen studs, and coated with gold-palladium prior to viewing with an ETEC "Autoscan" scanning electron microscope operated at 10 kv.

Transmission Electron Microscopy. All tissue preparation was conducted at 4 C unless otherwise indicated. Segments of seed coat one mm^2 were dissected from freshly harvested seeds while submerged in 5% (v/v) glutaraldehyde containing 100 mM phosphate buffer (pH 7.0). Segments were held under vacuum in the fixative for 24 h. Following vacuum infiltration, tissue samples were rinsed for 15-min three times in the same buffer and then postfixed 1 h with 1% (v/v) osmium tetroxide in Palade's buffer (16). The fixed tissue was dehydrated through 15-min steps of 50, 70, 95 (3×), and finally 100% ethanol (3×), followed by two 15-min changes of propylene oxide. The samples were held overnight at room temperature in a 1:1 mixture (v/v) of propylene oxide and resin (Polysciences "Poly-Bed 812/Araldite 502") and the following day embedded in resin ("Poly-Bed 812 Data Sheet," Polysciences, Warrington, PA) and hardened at 60 C for 48 h. To facilitate ultrathin (80–90 nm) sectioning, tissues not involved in photosynthate transport were carefully trimmed from the block. These included the cutinized epidermal palisade and hypodermal "hourglass" cell layers whose thick cell walls provide structural support for the seed. Thin sections were cut with glass knives on a Porter-Blum ultramicrotome. Those showing gold or silver interference colors were picked up on copper grids and examined in a Zeiss EM9A electron microscope. Selected sections were stained with alcoholic uranyl acetate (5%, w/v, in 50% methanol; 20 min at room temperature) and Reynold's lead citrate (10 min at room temperature) prior to photographing. The preliminary block trimming and the use of thicker sections than desired were necessary because the heterogeneous seed coat tissues often sectioned poorly.

Light Microscopy. To view the reticulate venation, lyophilized seed coats were repeatedly extracted with boiling 80% ethanol (1 h three times) and water (0.5 h once). Starch was subsequently removed by incubating the seed coats at 45 C for 44 h in 0.5% (w/v) glucoamylase in 0.1 N acetate buffer (pH 4.5). Tissues were carefully separated along two natural planes of weakness between the hourglass hypodermis, the parenchyma, and endothelium. Oblique hand sectioning of the isolated parenchyma layer followed by staining with 0.5% (w/v) aqueous toluidine blue allowed visualization of intact vascular bundles. With bright field micros-

[1] Present address: Central Research and Development Department, Experimental Station, E. I. du Pont de Nemours and Co., Wilmington, DE 19801.

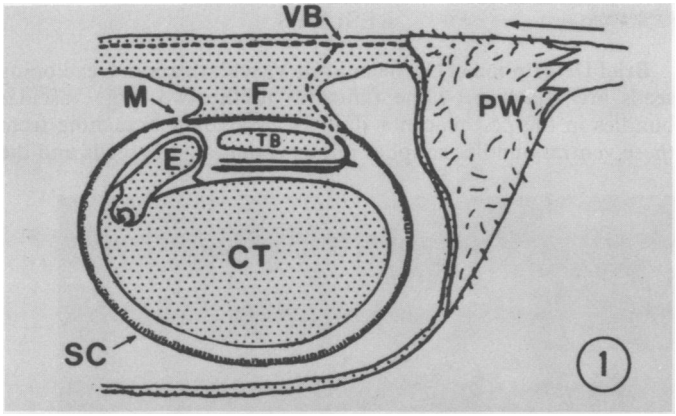

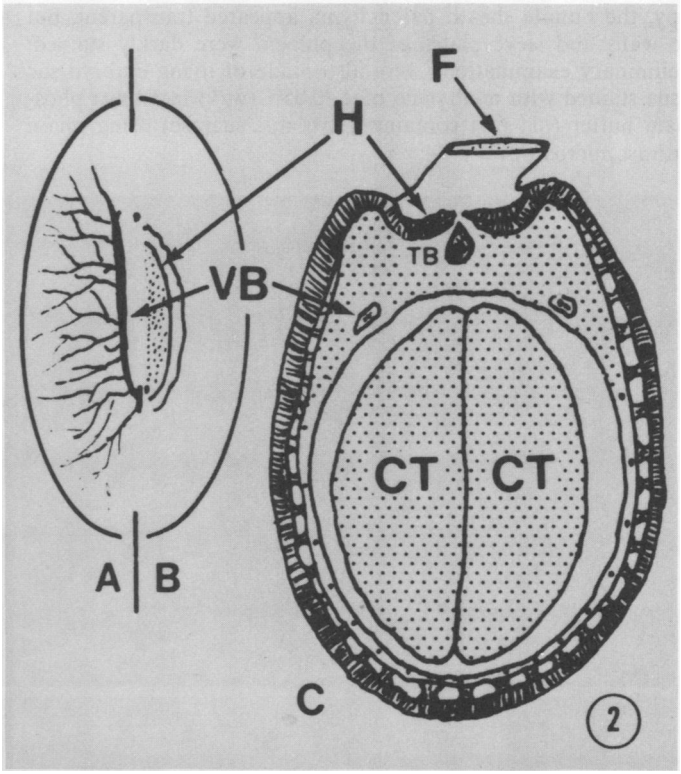

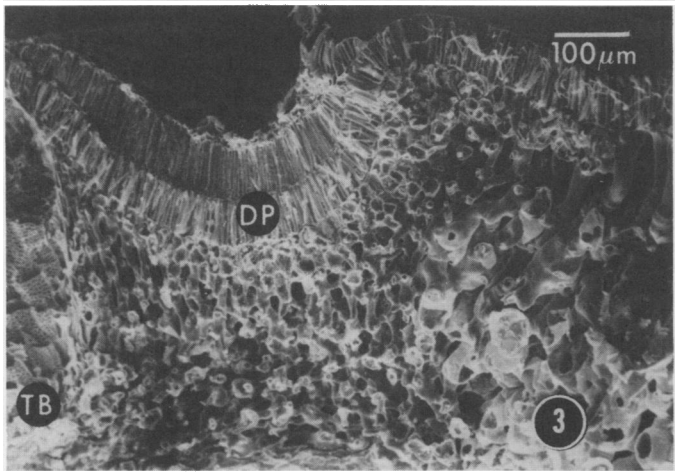

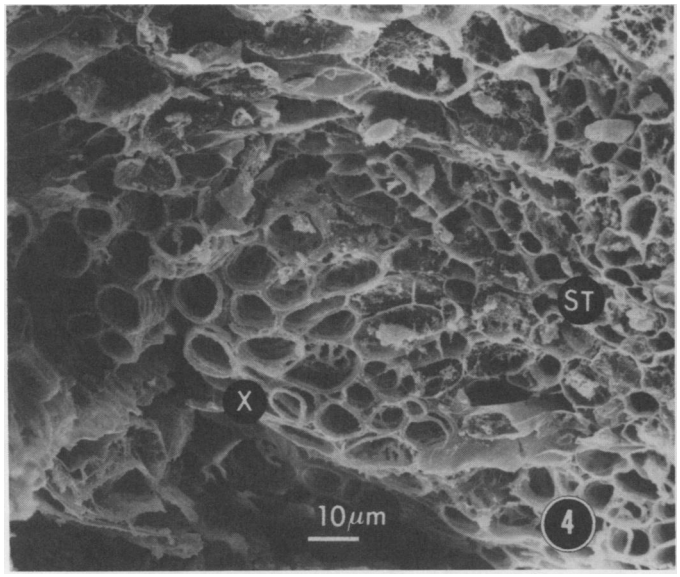

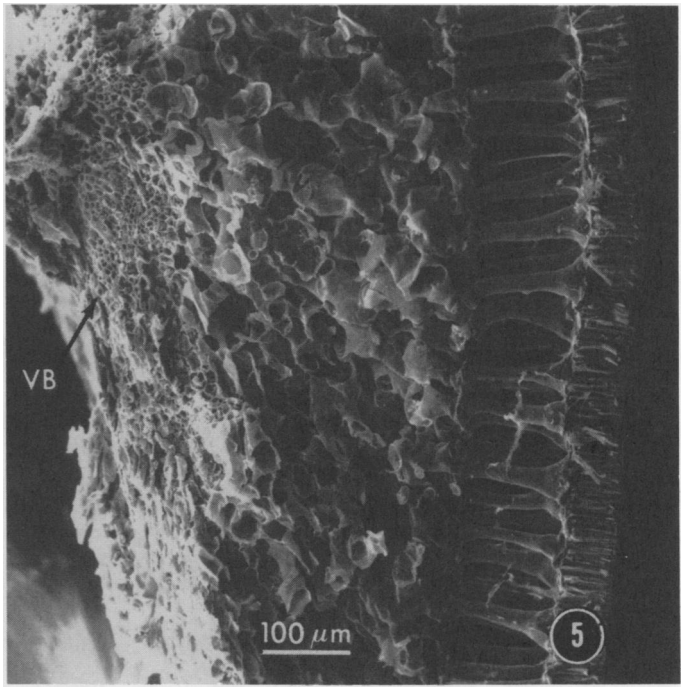

FIGS. 1 to 5. Anatomy of soybean seed attachment and vascularization of the seed coat. CT, cotyledon; DP, double palisade of the hilum; E, embryonic axis; F, funiculus; H, hilum; M, micropyle; PW, pod wall; SC, seed coat; ST, phloem sieve tubes; TB, tracheid bar; VB, vascular bundles; X, xylem.

FIG. 1. Sketch of a typical median sagittal section of an entire seed attached by the funiculus to a ventral bundle of the pod. A single vascular bundle enters the seed coat at the chalazal end of the hilum and branches below the tracheid bar to form two lateral bundles.

FIG. 2. Vascularization of the soybean seed coat. A, sketch of a lateral bundle, illustrating the approximate relationship to the hilum, illustrated in (B). The initial branching of the reticulate venation is also illustrated in (A). C, sketch of a typical transverse section of an entire seed attached to the funiculus, illustrating the approximate location of the lateral vascular bundles in relation to the tracheid bar, hilum, and cotyledons.

FIG. 3. SEM of the right half of the hilum region illustrated in Figure 2C. Shown are the tracheid-like cells of the tracheid bar, the double palisade layer forming the hilum epidermis, and the small parenchyma cells of the hilum region.

FIG. 4. SEM of lateral vascular bundle, composed of phloem sieve tubes and lignified xylem elements.

FIG. 5. SEM of a portion of the soybean seed coat illustrated in Figure 2C, relating the size and location of the lateral vascular bundle from Figure 4.

copy, the bundle sheath parenchyma appeared transparent, but the walls and sieve plates of the phloem were darkly stained. Preliminary examinations were also made of living embryo sac tissue stained with methylene blue (0.05% (w/v) in 50 mM phosphate buffer (pH 6.5) containing 100 mM sucrose) using phase contrast microscopy.

RESULTS

Brief Description of Soybean Fruit Vascularization. Developing seeds are attached by the funiculus to the two large vascular bundles in the pod placenta (Fig. 1). Secondary branching from these ventral bundles supplies photosynthate to the seeds and the

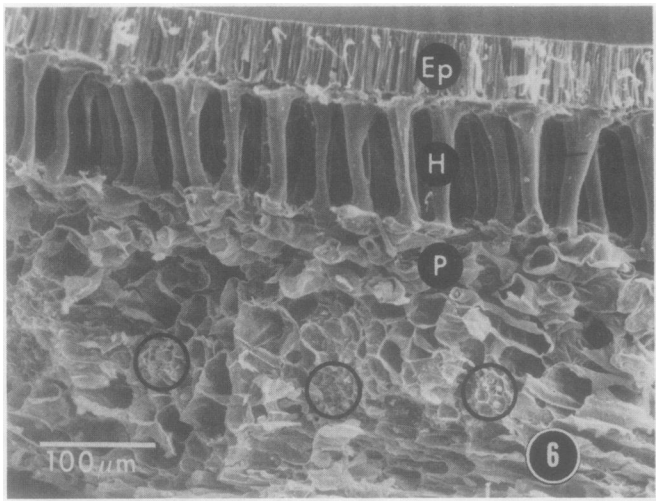

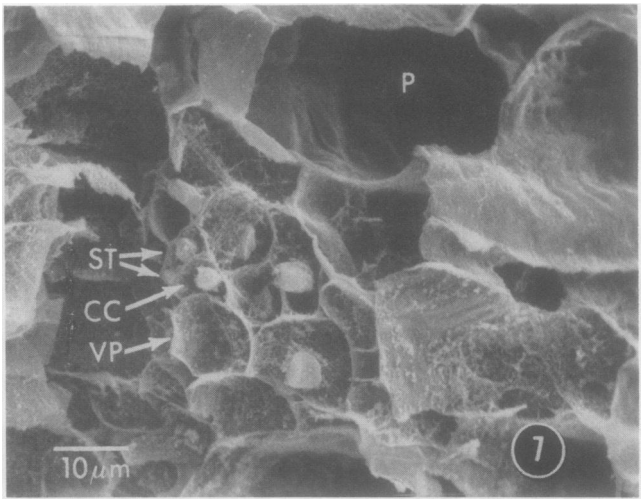

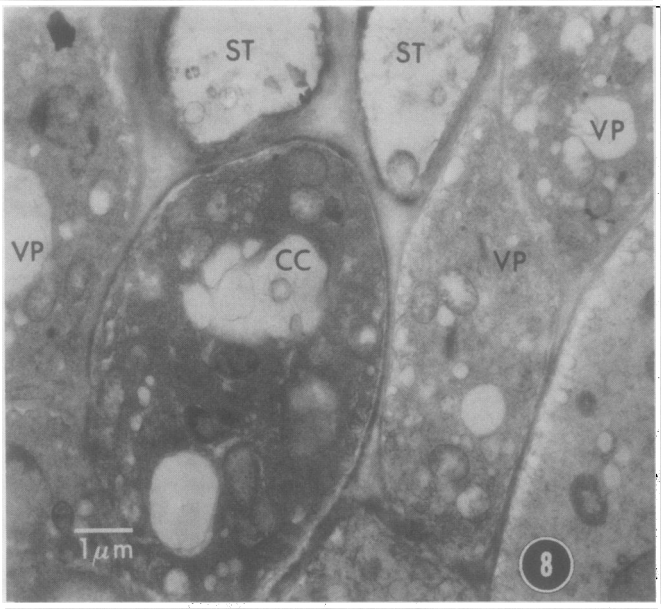

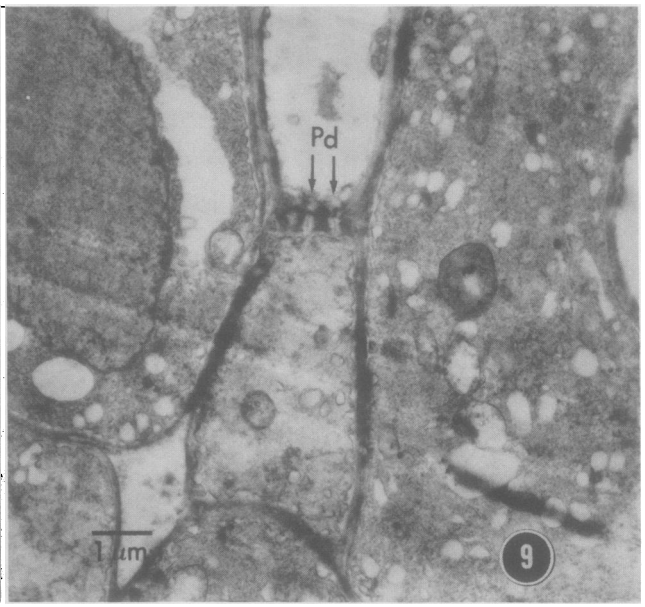

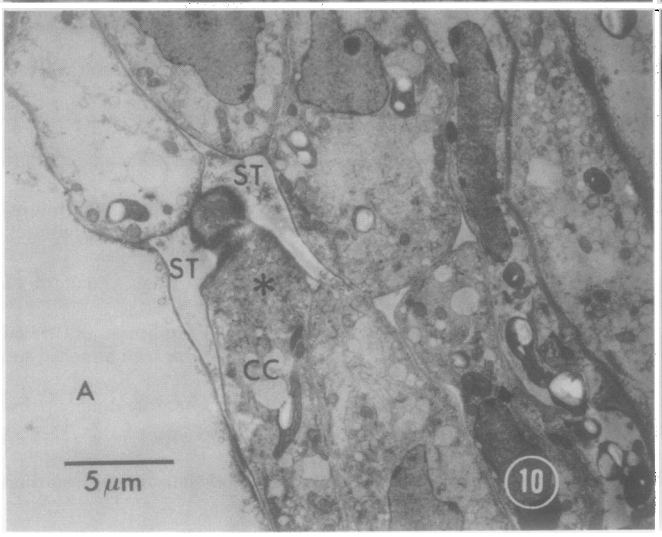

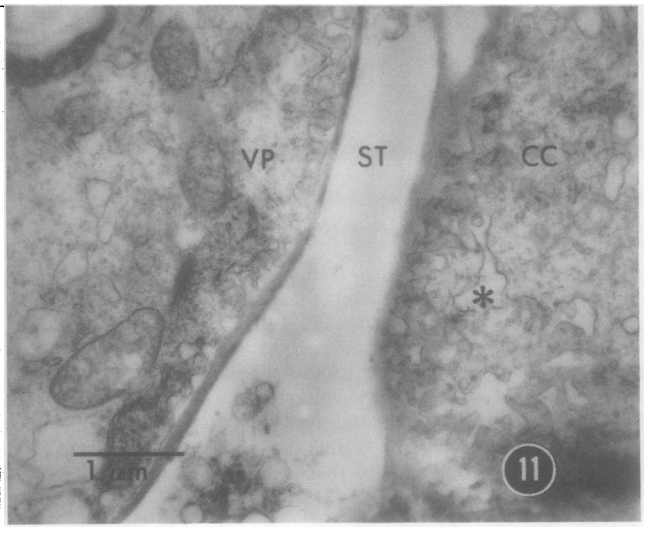

pod walls. Although the pod walls are extensively vascularized, only a single branch bundle enters each seed. This bundle passes through the funiculus and enters the seed at the posterior end of the hilum. There it joins at nearly right angles two parallel bundles which extend the length of the hilum near the inner surface of the seed coat (Figs. 1 and 2). Along these two large bundles, numerous smaller bundles depart from each, anastamosing repeatedly within the seed coat (Fig. 2A). Photosynthate exiting these minor bundles must apparently move intercellularly through the seed coat to the surface of the enclosed embryo. No vascular connections exist, however, between the seed coat and the cotyledons of the developing embryo (Fig. 2C). They are, in fact, separated by a thin maternal tissue, the embryo sac.

ANATOMY OF SEED COAT TISSUES

The Hilum. The hilum region of the seed coat (Fig. 2B) is composed of several distinct tissues, few of which are involved in photosynthate import. At the hilum, the seed coat is considerably thicker (Fig. 2C) and exhibits marked cellular differences from the remainder of the seed coat. The palisade at the hilum of a detached seed is double (Fig. 3), actually composed of the true epidermis of the seed and also a similar layer torn from the funiculus during separation of the seed from the pod placenta (17). A longitudinal cleft in the hilum divides the double palisade and exposes the tracheid bar. This bar is an elongated cluster of nonvascular tracheid-like cells (Fig. 3) thought to function as a water reservoir at times during seed development (17). Parenchyma cells of the hilum region are much smaller than those of the remainder of the seed coat (Fig. 3).

The two lateral vascular bundles (Figs. 1 and 2) can be seen in transverse section (Fig. 4) to be composed of both phloem and xylem elements. There are approximately the same number of xylem elements in these bundles as in the median bundle as it enters the seed; however, the amount of phloem is much less. These large lateral bundles are found deep within the seed coat (Figs. 1 and 2), just below a layer of irregularly shaped, interconnected parenchyma (Fig. 5). Above this layer, the cells of the hypodermis are hourglass-shaped and elongated approximately 120 μm perpendicular to the seed surface (Figs. 5 and 6). The unevenly thickened cell walls are thin at the ends of the cell and very thick in the central, constricted portion, thus forming a strong supporting layer with considerable intercellular space. Finally, the epidermal layer (Fig. 6) consists of closely-packed palisade cells. These spindle-shaped cells are elongated approximately 50 μm perpendicular to the seed surface, have thickened, pitted walls in the upper part of the cell, and contain numerous starch-containing chloroplasts. By maturity these cells are reportedly fully cutinized, providing a strong, gas-impermeable surface (2).

Seed Coat Reticulate Venation. Originating from the two lateral vascular bundles below the hilum is an extensive vascular system, formed when 10 to 15 minor bundles depart from each large lateral bundle (Fig. 2A) and anastamose repeatedly throughout a narrow zone in the parenchyma layer of the seed coat (Fig. 6). They extend almost completely around either side of the seed, so that the entire seed coat is vascularized (Fig. 2A) except in the region over the embryonic axis at the micropyle (Fig. 1).

The reticulate venation is composed of small, thick-walled sieve tubes surrounded by a bundle sheath of small vascular parenchyma cells (Fig. 7). Xylem tissue is conspicuously absent. Sieve element size and number per bundle diminishes markedly with distance from their origin at the lateral bundles below the hilum. Apparently there are no fewer than two files of sieve tubes per bundle, and near the hilum as many as eight were observed. Sieve element size decreases from about 450 μm to less than 200 μm in length, and from about 15 μm to less than 5 μm in diameter. Those within or adjacent to lateral anastamoses are 40 to 50% shorter than others nearby. A lateral anastamosis between two files of sieve tubes requires additional sieve plates in lateral walls at the junctures.

Within the minor bundles of the reticulate venation, the sieve tubes are symplastically associated by plasmodesmata with the dense cytoplasm of contiguous companion cells (Figs. 8 and 9). It is unknown whether these cells are companion cells in a strict ontogenetic sense (*i.e.* developing simultaneously with the SE[2] from the same phloem cell [5]), but they are considerably longer and darker staining than other vascular parenchyma cells (Figs. 8 and 10). In some glancing tangential sections, cell wall ingrowths were observed in the CC (Fig. 11).

The small vascular parenchyma cells of the bundle sheath are distinctively smaller than the nonvascular parenchyma tissues in which they are embedded (Fig. 10). They are much less cylindrical than the CC, and contain a variably dense cytoplasm (Figs. 8 and 10). In some cases, the cytoplasm contains primarily a large vacuole, while in others the cytoplasm is dense, and contains a reduced vacuole, extensive dictyosome activity, many vesicles, RER, elongated mitochondria, and leucoplasts (Figs. 8 and 10). Often present in these cells is a large, invaginated nucleus with conspicuous chromatin masses and multiple nucleoli. The cells of the bundle sheath are interconnected by abundant plasmodesmata.

Seed Coat Parenchyma. The reticulate venation of the seed coat is imbedded within a narrow zone separating two distinctly different parenchyma tissues. Directly above the level of vascularization are several layers of articulated parenchyma extending approximately 100 μm below the hourglass hypodermis layer (Figs. 6 and 12). Thick cell walls delineate these large, irregularly-shaped cells, but abundant plasmodesmata span the thin walls at points of cellular interconnection (Fig. 13). Intercellular spaces are extensive as a result of the structural asymmetry. These cells possess a dense cytoplasm enriched in constituents characteristic of cells engaged in active carbohydrate transport and excretion

[2] Abbreviations: SE, sieve element; CC, companion cell; SE-CC, sieve element-companion cell; SEM, scanning electron micrograph; TEM, transmission electron micrograph.

FIGS. 6 to 11. Anatomy and ultrastructure of seed coat reticulate venation. A, aerenchyma cell; CC, companion cell; Ep, epidermal cells; H, hypodermal, or hourglass cells; P, parenchyma cells; Pd, plasmodesmata; ST, sieve tube; VP, vascular parenchyma cell.

FIG. 6. SEM of a seed coat portion illustrating the reticulate venation (circled) embedded within the parenchyma layer. The distinctive spindle-shaped cells of the epidermis and hourglass-shaped cells of the hypodermis provide structural support to the seed.

FIG. 7. Detail of one of the vascular bundles circled in Figure 6. The smooth internal cell walls of the nonvascular, articulated parenchyma contrasts sharply to the internal walls of the companion and vascular parenchyma cells.

FIG. 8. TEM through a small bundle of the reticulate venation. Two contiguous thick-walled sieve tubes border a darkly-stained companion cell, and are flanked by several vascular parenchyma cells. The diameter of the sieve tubes within the reticulate venation is considerably smaller than those found in the vascular tissue of the vegetative soybean plant.

FIG. 9. Plasmodesmata (arrows) connect the cytoplasm of a companion cell with the lumen of a sieve tube.

FIG. 10. Tangential TEM section through a small bundle of the reticulate venation near a point of anastamosis of two sieve tube files. The cytoplasmic density and small size of the cells of the vascular bundle contrast sharply with the adjacent aerenchyma cell. The asterisk indicates a glancing longitudinal section through a companion cell.

FIG. 11. TEM of a companion cell and vascular parenchyma cell straddling a sieve tube element. This glancing longitudinal section of the companion cell reveals wall ingrowths (asterisk) otherwise concealed by the dark-stained cytoplasm. These ingrowths were apparently associated with the cell wall (in the plane of the picture) that was removed in the previous serial section. Ingrowths appear white, surrounded by darker plasmalemma and cytoplasm.

(12); large, irregularly-shaped nuclei; and abundant RER, dictyosomes, vesicles, and mitochondria (Figs. 13 and 14). Distinctive paramural antibodies (13) are present (Fig. 15).

Below the level of seed coat vascularization, the parenchyma is composed of 10 to 15 layers of thin-walled aerenchyma cells, all interconnected to form a three-dimensional lattice (Fig. 16). The cytoplasm of this aerenchyma is nearly devoid of organelles. The lattice apparently forms a continuous apoplastic route from the vascular plane to the inner seed coat surface. These aerenchyma cells are easily observed because their tangential interconnections are delicate, and a natural fault line facilitating dissection occurs at the junction of the aerenchyma and the endothelium (Fig. 17).

Ultrastructure of the Endothelium. The inner surface of the seed coat, the endothelium or integumentary tapetum, is formed by a single layer of small, thick-walled cells (Fig. 18). Pamplin (17) considers this seed coat layer to have differentiated from the inner integument 10 to 14 days after flowering. This study supports his conclusion, for it is clearly outside the embryo sac which enclosed the endosperm prior to its absorption by the embryo (7, 17, 21). Thus, it seems that the endothelium cannot be a remnant of the cellular endosperm, as some sources suggest (2, 5, 21, 24, 25).

The endothelial cells possess an unusually dense cytoplasm, with a reduced vacuole and nucleus but are distinctively enriched with mitochondria, ribosomes, dictyosomes, vesicles, and extended, tubular RER (Figs. 19 and 20). No leucoplasts or starch were observed. The thick cell walls of this endothelial layer form the smooth inner surface of the seed coat. No pores, plasmodesmata, or vascular tissue exist to carry photosynthate to the embryo from the surrounding endothelium.

ANATOMY OF THE EMBRYO SAC

Between the embryonic cotyledons and the seed coat is the embryo sac, also maternal tissue. The morphology and ultrastructure of this tissue as it appears during early embryogenesis in other species has been partially described (14, 15, 19). In the present study, the embryo sac consisted of a single layer of multicellular tubules, each 50 × 200 to 350 μm, attached at one end to form an undulating surface facing the seed coat (Fig. 21). In young seeds the tubules probably project into the endosperm that they enclose, but as the cotyledons develop they are progressively flattened (Fig. 22). The cell walls of the seed coat endothelium and those of the embryo sac are tightly appressed to each other, but they are not fused, and there are no connecting plasmodesmata (Fig. 22).

Cross walls bearing abundant plasmodesmata separate each tubule into several cells, each distinctly different with respect to cytoplasmic density (Fig. 23). Near the seed coat, the cytoplasm is similar to that of the endothelium (Fig. 22), although the tubular RER is notably absent. Numerous mitochondria, ribosomes and short RER segments, leucoplasts, dictyosomes, and vesicles are present, often restricted to a thin peripheral layer of dense cytoplasm by a large, invaginated nucleus that has several distinctive chromatin masses. Conversely, the vestigial cytoplasm of the central region of the tubules contains only a small amount of RER, occasional mitochondria, and numerous developing vacuoles (Fig. 22). A final cross wall defines the small terminal portion of the tubules. Although the cytoplasm of this terminal region is notably devoid of most organelles, abundant plasmodesmata link it with dense cytoplasm near the distal end of the preceding cell (Fig. 23). This cytoplasm, like that of the region near the endothelium, is often enriched in those constituents characteristic of cells involved in active carbohydrate transport or secretion (12).

THE EMBRYONIC COTYLEDONS: A PREVIEW

The embryonic cotyledons are the ultimate sink for imported photosynthate. The epidermal cells forming the surface of the cotyledons are not symplastically connected to the embryo sac or seed coat. These epidermal cells are many times smaller than the embryo sac tubules that they face, and lack the extensive accumulations of protein and oil of the mesophyll parenchyma cells immediately below (Fig. 24). The adjacent pentagonal mesophyll cells are usually attached to each other at five sites around the cell perimeter as well as above and below in each cell file (Fig. 25). Large intercellular spaces created by this orderly arrangement probably facilitate gas exchange. The ultrastructure of the embryonic cotyledons, with respect to photosynthate absorption and utilization, will be considered in another paper.

DISCUSSION

GENERAL CONSIDERATIONS

The results of this study show the maternal seed coat to be a complex body of many contrasting cell types. Because of their unique shapes (Fig. 6) and physical contribution to seed dormancy (2), the epidermal and hypodermal "hourglass" cells have traditionally received most cytological attention. Although there are substantial amounts of starch in these cells (micrographs not shown), it seems unlikely that they make a significant contribution to the nutrition of the embryo in any direct manner. This is not to conclude, however, that there is no interaction between the embryo and the structural cells during this period. By limiting O_2 availability the epidermal cells may exert some effect on potential photosynthate import.

Perhaps a more significant role is played by the large, articulated parenchyma cells (Fig. 12) directly above the vascular zone of the seed coat (Fig. 6). The dense cytoplasm of these cells (Figs. 13 and 14) suggests intense metabolic activity, for large numbers of polysomes, active dictyosomes, and secretion vesicles were observed (Fig. 14). Many of the vesicles were free, but others were in close proximity to an invaginated plasmalemma. Given the persistent photosynthate metabolism needed to maintain rapid embryo growth, it is tempting to speculate on a role for these seed coat tissues in the refixation of CO_2 respired by the embryo. The only support available for this hypothesis is the presence of high PEP carboxylase activity in *Pisum* seed coats during this developmental period (8).

PROBABLE PATHWAY OF PHOTOSYNTHATE IMPORT

The results of this and recent (22, 23; Thorne, unpublished) studies of soybean seed development have provided us with a clear picture of the probable route followed by photosynthate through maternal seed tissues to the developing embryo (Fig. 26). Less is known of the molecular mechanisms of sugar fluxes along this route. The following conceptual model, supported by anatomical and physiological data, may present a partial explanation.

Phloem Unloading. Phloem translocation of imported photosynthate ceases within the seed coat reticulate venation (23). The removal of photosynthate from the sieve tubes of the reticulate venation is probably accomplished through unloading by the CC (Fig. 8). These are symplastically linked to the phloem lumen by plasmodesmata to form a SE-CC complex (Fig. 9). In leaves, these cytoplasmic connections exclude organelles from the phloem but maintain similar solute concentrations and, thus, turgor pressures in both the sieve tubes and companion cells (6). If unloading *from* the SE-CC complex within the seed coat is the reverse of active loading *into* the SE-CC complex in leaves (6), photosynthate withdrawn from the seed coat phloem would be transported from the CC symplast to its cell wall apoplast by carrier systems located in the plasmalemma. Conversely, unloading from the seed coat phloem could occur passively, down a concentration gradient into the aerenchyma apoplast. While the unloading process is energy-dependent (Thorne, unpublished), the basis for this dependency has not been established. It is tempting to speculate that the

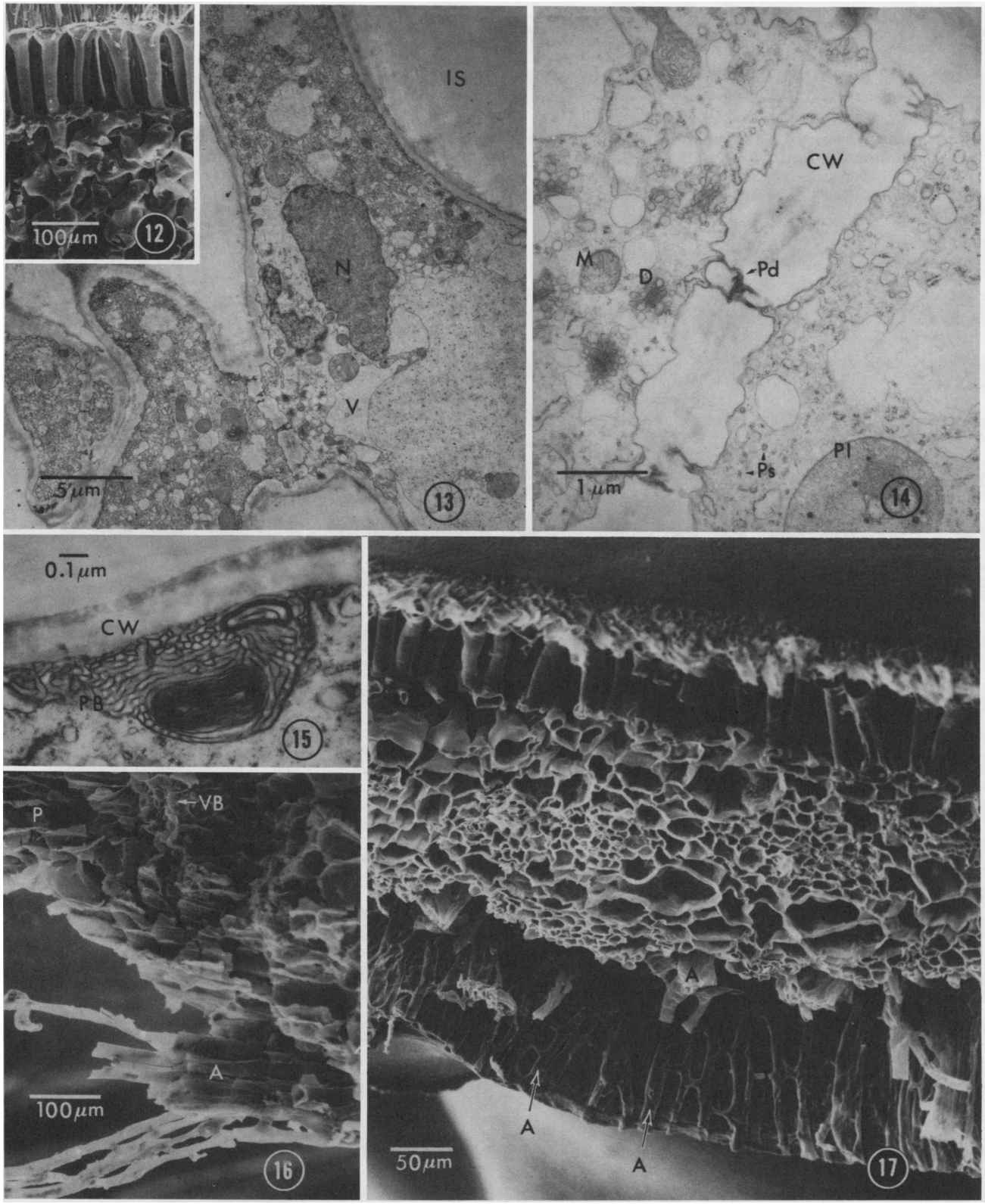

FIGS. 12 to 17. Morphology and ultrastructure of the two types of parenchyma: articulated Figures 12 to 15; aerenchyma, Figures 16 and 17. A, aerenchyma; CW, cell wall; D, dictyosome; IS, intercellular space; M, mitochondrion; N, nucleus; P, parenchyma; PB, paramural body; Pd, plasmodesmata; Pl, plastid; Ps, polysomes; V, vacuole; VB, vascular bundle.

FIG. 12. SEM of the outer layers of a seed coat, illustrating the articulated parenchyma, the ultrastructure of which is examined in Figures 13 to 15.

FIG. 13. TEM showing the ultrastructure of typical cells of the articulated parenchyma. The irregular shapes of these cells produce large intercellular spaces. External cell walls are often much thicker than those at points of cellular connection. The dense cytoplasm usually contains a large nucleus but a reduced vacuole.

FIG. 14. Detail of Figure 13 showing numerous plasmodesmata spanning points of cellular connection. The cytoplasm of these cells closely resembles that of actively secreting nectary cells. They possess reduced vacuoles and dense cytoplasm, with numerous mitochondria, active dictyosomes, and large, irregular nuclei.

FIG. 15. TEM of highly-developed paramural body near an outer wall of the articulated parenchyma.

FIG. 16. SEM of the inner layers of a seed coat, illustrating the tubular aerenchyma cell layers, interconnected to form a three-dimensional lattice. Near the top of the micrograph is an obliquely-fractured vascular bundle, embedded in the zone of transition between parenchyma cell types.

FIG. 17. SEM of an entire seed coat section, the endothelium peeled down to expose the innermost layer of attached aerenchyma cells.

observed CC wall ingrowths (Fig. 11) indicate the presence of transfer cells and serve to enlarge the area of the plasmalemma, the number of putative membrane carrier sites, and the flux of photosynthate from the SE-CC complex (18). Plasmodesmata link the cytoplasm of the companion cells to that of the surrounding vascular parenchyma cells (micrographs not shown). The combined unloading capacity of both plasmalemma surfaces and the intricacy of the aerenchyma lattice are perhaps responsible for the rapid import of photosynthate by the seed coat (23). However, the cellular events associated with the unloading of photosynthate

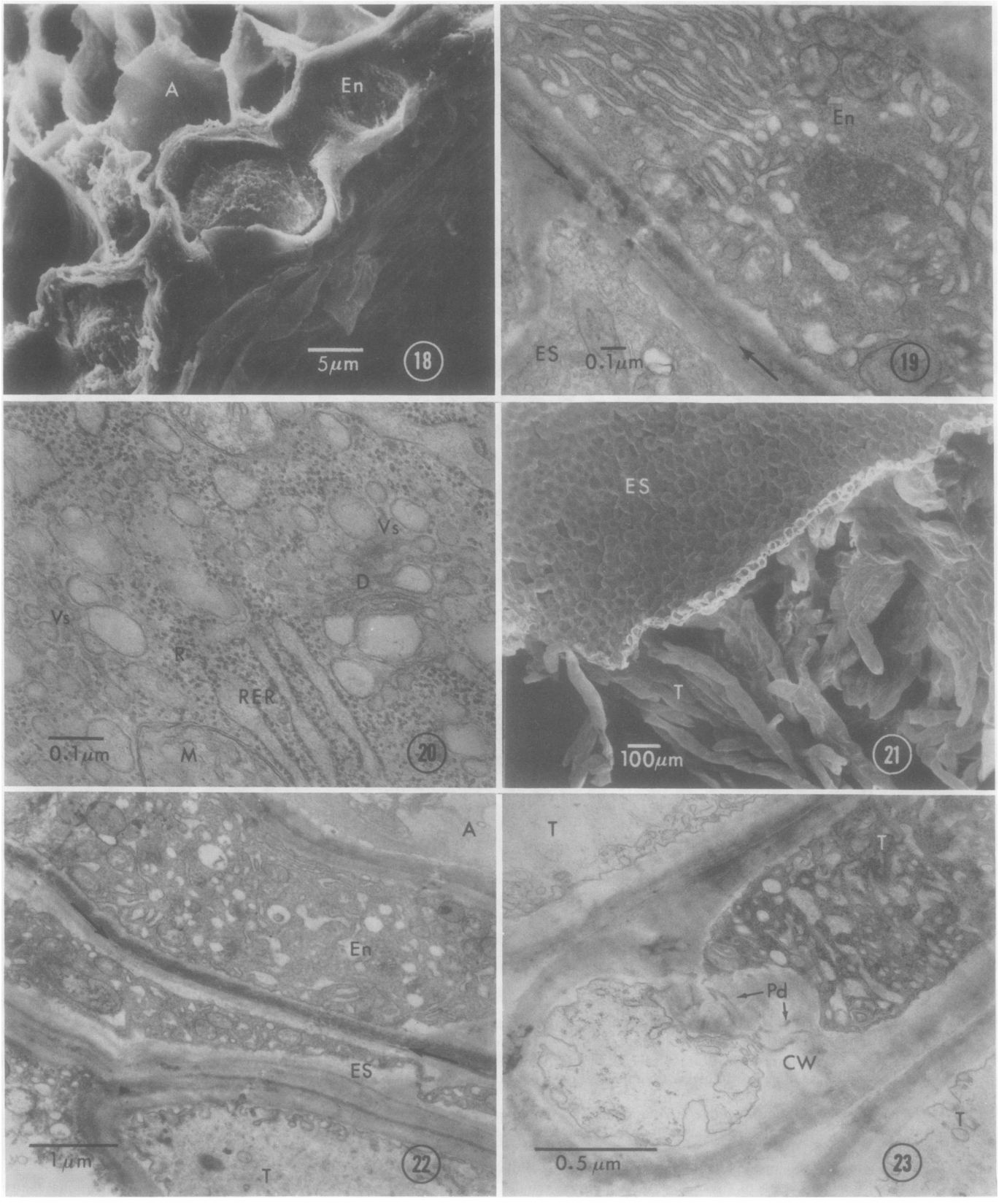

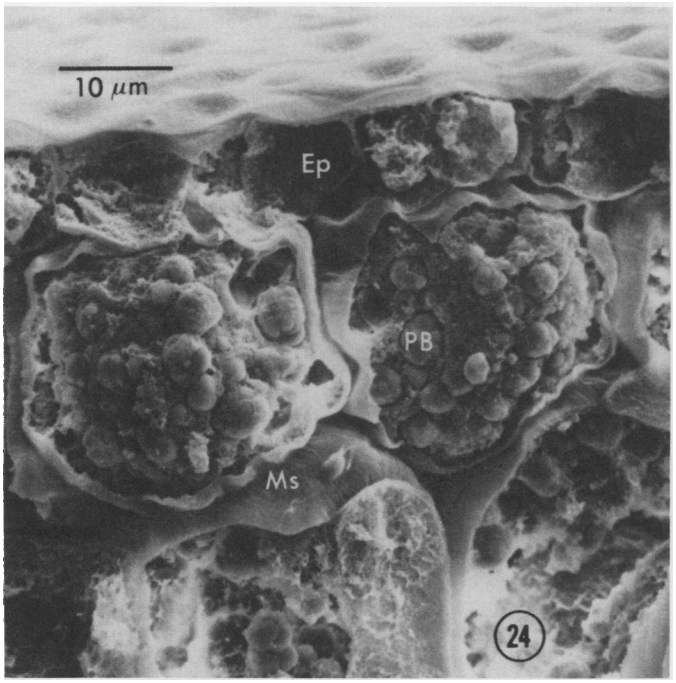

FIG. 24. Morphology of the soybean cotyledon. SEM of the outer abaxial cell layers of a 50-day-old soybean cotyledon. The small epidermal cells lack the extensive accumulations of lipid and protein bodies of the mesophyll parenchyma cells below. Ep, epidermal cells; PB, protein bodies; Ms, mesophyll parenchyma cells.

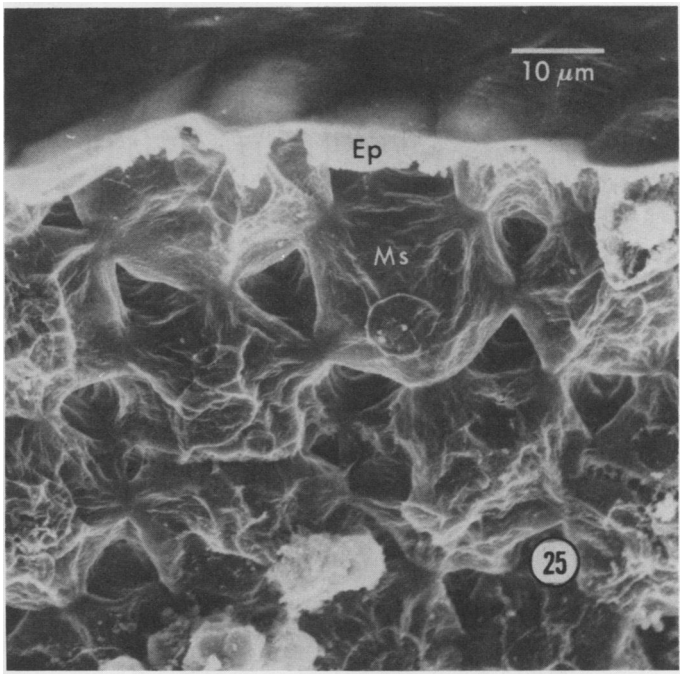

FIG. 25. Morphology of the soybean cotyledon. SEM illustrating the large intercellular spaces created by the stacked arrangement of pentagonally-shaped mesophyll parenchyma cells. Ep, epidermal cells; Ms, mesophyll parenchyma cells.

from sieve tubes have received little attention and are poorly understood.

Intercellular Transport. Following unloading, photosynthate traverses the layers of the aerenchyma tissue (Figs. 16 and 17) before release from the inner surface of the seed coat (Fig. 18). These interconnected aerenchyma cells with their conspicuously large intercellular spaces, are characteristic of plants growing in wet, O_2-deficient habitats, not totally unlike that experienced deep within the tissues of the fruit. Ostensibly, the physiological advantage of the large intercellular spaces of these cells is to facilitate O_2 movement through the seed coat to the embryo (10^4-fold faster diffusion in intercellular air than when dissolved in water within the cell walls).

A symplastic transport route through the aerenchyma following unloading from the phloem is not likely, for (a) the highly vacuolated cells lack the numerous mitochondria, dictyosomes, and other components characteristic of granulocrine secretion in other systems (solute confined within vesicles of dictyosome origin); (b) sucrose, the principal photosynthate, traverses the seed coat without the extensive metabolism that would be expected if it were within the symplasm but uncompartmented; and (c) rate of transport across the seed coat following unloading is slow, as though by diffusion (23).

Conversely, it is not difficult to envision an apoplastic route for intercellular transport of photosynthate through the seed coat aerenchyma following unloading from the phloem. It would likely occur as diffusion down a concentration gradient, established at one end of the system by phloem unloading and maintained at the other end by active photosynthate accumulation or utilization by the embryo. Although an apoplastic route undoubtedly restricts the total capacity of a transport system (9), the environmental sensitivity of the processes at either end of this system (Thorne, unpublished) apparently exerts primary control over seed coat transit time, and photosynthate availability for embryo growth.

Elimination from the Seed Coat. It is difficult to envision adequate maternal control of photosynthate delivery to the embryo with an uninterrupted apoplastic route after phloem unloading. For reasons of osmotic or developmental control, it would seem to be advantageous to maintain isolation between maternal and embryonic tissues. Apparent wall incrustations of electron-dense material observed between adjacent endothelial cells may

FIGS. 18 to 23. Morphology and ultrastructure of the seed coat endothelium (Figs. 18–20) and the embryo sac tubules (Figs. 21–23). A, aerenchyma cell; CW, cell wall; D, dictyosome; ES, embryo sac; En, endothelium; M, mitochondrion; Pd, plasmodesmata; R, ribosomes; RER, rough endoplasmic reticulum; T, tubule; Vs, vesicles.

FIG. 18. SEM of the endothelial cell layer forming the inner surface of the seed coat. Several layers of the aerenchyma lattice are present above this layer.

FIG. 19. Ultrastructure of a typical endothelial cell. Extensive tubular RER dominate the dense cytoplasm. Arrows indicate the apoplast boundary formed where the inner surface of the seed coat and the base of the embryo sac tubules are appressed, also seen in Figure 22.

FIG. 20. Detail of the dense endothelial cytoplasm showing the characteristic mitochondria, dictyosomes, ribosomes, tubular RER, and vesicles.

FIG. 21. SEM of a soybean embryo sac, illustrating the very large multicellular tubules, fused at one end to form a porous, undulating embryo sac base surface (ES) facing the seed coat. The tubules appear pendent as a result of tissue preparation but are normally flattened in maturing seeds by the enlarging cotyledons, as in Figure 22.

FIG. 22. Ultrastructure of the embryo sac base surface (ES) in place against the inner, endothelial (En) surface of the seed coat and, above it, the aerenchyma (A). Near the base, the cytoplasm of the tubule (ES) is nearly as dense as the endothelium that it faces. But a short distance from the base, perhaps in another cell of the same tubule, the tubule cytoplasm (T) is nearly devoid of organelles.

FIG. 23. Ultrastructure of three adjacent tubules, illustrating the unusual tip region in the center tubule and the vacuolated regions of two others. Abundant plasmodesmata span the cell walls dividing the tubules into cells or cellular sections.

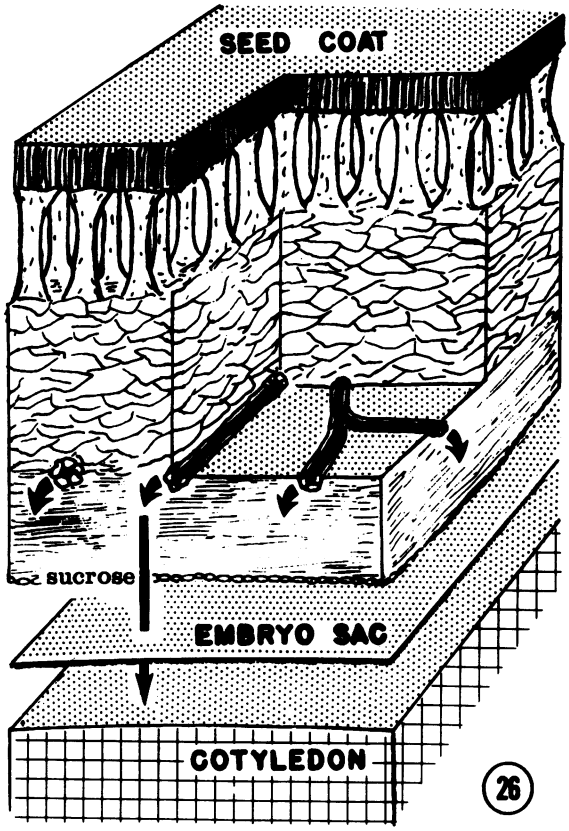

FIG. 26. Schematic overview of the apparent route of sucrose import from the sites of unloading within the seed coat to the embryonic cotyledons. Relative cell sizes within the seed coat are approximate.

effectively block a continuous apoplastic pathway (micrographs not shown). If so, the release of photosynthate may require passage through the symplasm of the endothelial layer. Indeed, these cells are striking in their appearance: thick cell walls, capable of withstanding the turgor pressure that an accumulating cell could develop, and dense cytoplasm with numerous mitochondria, ribosomes, dictyosomes, vesicles, and extended, tubular RER (Figs. 19 and 20). The morphology and ultrastructure of these cells have not been previously reported. Pate and Gunning (18) have reported that the endothelial cells of *Vicia* and *Lathyrus* species (but not *P. vulgaris*) may be modified to transfer cells, and thus supply nutrient to the embryo in a facilitated manner. In soybean, however, the endothelial cells more closely resemble cells of secreting glands of *Arctium*, *Petunia*, and *Typhonium* (12) because of their extensive tubular RER and absence of the cell wall ingrowths typical of transfer cells. It is unknown if the similarity has a physiological basis.

Passage through the Embryo Sac. The morphology, ultrastructure, and function of the embryo sac in soybean seeds nearing maturity have not been previously described. Studies of this tissue in other species (7, 14, 15, 19) have noted the presence of embryo sac wall ingrowths during early embryogenesis. They failed to observe the presence of multicellular tubules, perhaps due to species and/or ontogenetic differences in embryo sac anatomy. Certainly the examination by SEM of the intact tissue when removed from the seed facilitated this observation in the present study. For example, while unreported in the paper, the morphology of the soybean embryo sac with respect to the endothelium (integumentary tapetum) and the 8-day-old embryo can be observed in Carlson's figure 170 (2). These earlier workers suggested that, because of its location, the embryo sac somehow aids the passage of nutrient to the embryo during the initial period of cotyledon growth but is crushed by the maturing embryo (7, 14, 15, 19). The results of this study do not support their latter conclusion. That these cells are alive weeks after the endosperm they enclosed was digested suggests that they may continue to play a role in the nutrition of the embryo. But, since the embryo sac base formed by the fused tubule ends appears to present a rather porous surface to the seed coat endothelium, photosynthate could possibly diffuse from the seed coat to the cotyledons without entering the embryo sac symplasm. The dense cytoplasm (Figs. 22 and 23), anatomical form (Fig. 21) and functional location of this tissue (Fig. 26) should stimulate further studies of its function.

Uptake by the Cotyledons. With the uptake of photosynthate by the embryonic cotyledons, the ultimate sink in this transport system, metabolism of the absorbed photosynthate can be rapid (23). Extensive formation of lipid and protein storage bodies (Fig. 24) characterize this period of development. Uptake by the embryo occurs from the apoplast surrounding the cotyledons (11, 23) since there is no symplastic connection between the maternal and embryonic tissues (23). The rate of uptake by excised immature cotyledons shows a biphasic dependence on external sucrose concentration (11; Thorne, unpublished). At low concentrations, uptake is dominated by a high affinity, saturable system; at concentrations greater than 25 to 50 mM, a low affinity, nonsaturable system becomes apparent. A sucrose-proton co-transport system has been demonstrated in developing soybean cotyledons (11).

Pate and Gunning (18) consider the small, epidermal cotyledon cells of some legume species to be transfer cells, with the absorption of photosynthate occurring at the cotyledon outer surface. Plasmodesmatal connections between adjacent cells (micrographs not shown) are consistent with this conclusion. The thick cell walls and abundant intercellular spaces (Fig. 25) also support the possibility of an apoplastic diffusion pathway, from which individual cells might actively accumulate photosynthate.

Acknowledgments—Many thanks are extended to Margaret O'Connell for expert technical assistance and Dr. A. Pooley of the Yale University SEM Laboratory for provision of facilities and assistance for SEM. The author is indebted to Dr. D. Aylor for many valuable discussions during the course of this and other studies.

LITERATURE CITED

1. ANDERSON TF 1951 Techniques for the preservation of three-dimensional structure in preparing specimens for the electron microscope. Trans NY Acad Sci Ser II 13: 130–134
2. CARLSON JB 1973 Morphology. *In* BE Caldwell, ed, Soybeans: Improvement, Production, and Uses, Chap 2. Am Soc Agron, Madison, WI, pp 17–95
3. CORNER EJH 1951 The leguminous seed. Phytomorphology 1: 117–150
4. DZIKOWSKI B 1937 Studia nad Soja *Glycine hispida* (Moench) Maxim. 11-ème partie. Anatomie. (French abstract) Pánstwowy Institut Naukowego Gospodarstwa Wiejstiege w Pulawach. Tom XVI. zeszyt 2. Rosprawa Nr 258: 261–265
5. ESAU K 1965 Plant Anatomy. John Wiley & Sons, New York, 767 pp
6. GEIGER DR Phloem loading. *In* MH Zimmerman, JA Milburn, eds, Transport in Plants. I. Phloem Transport. Encyclopedia of Plant Physiology. Springer-Verlag, Berlin, pp 395–431
7. HARDHAM AR 1976 Structural aspects of the pathways of nutrient flow to the developing embryo and cotyledons of *Pisum sativum* L. Aust J Bot 24: 711–721
8. HEDLEY CL, DM HARVEY, RJ KEELY 1975 Role of PEP carboxylase during seed development in *Pisum sativum*. Nature 258: 352–354
9. LÄUCHLI A 1976 Apoplastic transport in tissues. *In* U Lüttge, MG Pitman, eds, Transport in Plants. II. Part B, Tissues and Organs. Encyclopedia of Plant Physiology, Springer-Verlag, Berlin, pp 3–34
10. LE MONNIER MG 1872 Recherches sur la nervation de la graine. Ann Sci Nat Bot 16: 231–305
11. LICHTNER FT 1979 Sucrose/proton cotransport in developing soybean cotyledons. PhD thesis. Cornell University, Ithaca, New York
12. LÜTTGE U, E SCHNEPF 1976 Elimination processes by glands. Organic substances. *In* U Lüttge, MG Pitman, eds, Transport in Plants. II, Part B. Tissues and Organs. Encyclopedia of Plant Physiology, Springer-Verlag, Berlin, pp 244–277
13. MARCHANT R, AW ROBARDS1968 Membrane systems associated with the plasmalemma of plant cells. Ann Bot 32: 457–471
14. MARINOS NG 1970 Embryogenesis of the pea (*Pisum sativum*). I. The cytological environment of the developing embryo. Protoplasma 70: 261–279
15. NEWCOMB W, TA STEEVES 1971 *Helianthus anuus* embryogenesis: embryo sac wall projections before and after fertilization. Bot Gaz 132: 367–371

16. PALADE GE 1952 A study of fixation for electron microscopy. J Exp Med 95: 285–298
17. PAMPLIN R 1963 The anatomical development of the ovule and seed in the soybean. PhD thesis. University of Illinois, Urbana
18. PATE JS, BES GUNNING 1972 Transfer cells. Annu Rev Plant Physiol 23: 173–196
19. SCHULZ P, WA JENSEN 1974 *Capsella* embryogenesis: the development of the free nuclear endosperm. Protoplasma 80: 183–205
20. STEPHENSON RA, GL WILSON 1977 Patterns of asssimilate distribution in soybeans at maturity. The influence of reproductive developmental stage and leaf position. Aust J Agric Res 28: 203–209
21. STERLING C 1954 Development of the seedcoat of lima bean (*Phaseolus lumatus* L.). Bull Torrey Bot Club 81: 271–287
22. THORNE JH 1979 Redistribution of assimilates from soybean pod walls during seed development. Agron J 71: 812–816
23. THORNE JH 1980 Kinetics of ^{14}C-photosynthate uptake by developing soybean fruit. Plant Physiol 65: 975–979
24. WILLIAMS LF 1950 Structure and genetic characteristics of the soybean. *In* KS Markley, ed, Soybeans and Soybean Products, Vol 1. Interscience Publishers, New York, pp 111–134
25. WINTON AL 1906 The Microscopy of Vegetable Foods. Morphology of Organs. John Wiley & Sons, New York, pp 248–249